

---

# Tumor Uptake of Copper-Diacetyl-Bis(*N*<sup>4</sup>-Methylthiosemicarbazone): Effect of Changes in Tissue Oxygenation

Jason S. Lewis, Terry L. Sharp, Richard Laforest, Yasuhisa Fujibayashi, and Michael J. Welch

*Mallinckrodt Institute of Radiology, Washington University School of Medicine, St. Louis, Missouri; and Biomedical Imaging Research Center, Fukui Medical University, Matsuoka, Fukui, Japan*

---

We showed previously that, *in vitro*, copper-diacetyl-bis(*N*<sup>4</sup>-methylthiosemicarbazone) (Cu-ATSM) uptake is dependent on the oxygen concentration (pO<sub>2</sub>). We also showed that, *in vivo*, Cu-ATSM uptake is heterogeneous in animal tumors known to contain hypoxic fractions. This study was undertaken to confirm the pO<sub>2</sub> dependence of this selective uptake *in vivo* by correlating Cu-ATSM uptake with measured tumor pO<sub>2</sub>. **Methods:** Experiments were performed with the 9L gliosarcoma rat model using a needle oxygen electrode to measure tissue pO<sub>2</sub>. Using PET and electronic autoradiography, Cu-ATSM uptake was measured in tumor tissue under various pO<sub>2</sub> levels. The oxygen concentration within implanted tumors was manipulated by chemical means or by altering the inhaled oxygen content. **Results:** A good correlation between low pO<sub>2</sub> and high Cu-ATSM accumulation was observed. Hydralazine administration in animals caused a decrease in the average tumor pO<sub>2</sub> from 28.61 ± 8.74 mm Hg to 20.81 ± 7.54 mm Hg in untreated control animals breathing atmospheric oxygen. It also caused the tumor uptake of Cu-ATSM to increase by 35%. Conversely, in animals breathing 100% oxygen, the average tumor pO<sub>2</sub> increased to 45.88 ± 15.9 mm Hg, and the tumor uptake of Cu-ATSM decreased to 48% of that of the control animals. PET of animals treated in a similar fashion yielded time-activity curves showing significantly higher retention of the tracer in hypoxic tissues than in oxygenated tissues. **Conclusion:** These data confirm that Cu-ATSM uptake in tissues *in vivo* is dependent on the tissue pO<sub>2</sub>, and that significantly greater uptake and retention occur in hypoxic tumor tissue. Therefore, the possible use of Cu-ATSM PET as a prognostic indicator in the management of cancer is further validated.

**Key Words:** hypoxia; copper-diacetyl-bis(*N*<sup>4</sup>-methylthiosemicarbazone); oxygen measurement

**J Nucl Med 2001; 42:655–661**

---

**T**he presence of hypoxia within tumors can be correlated with a resistance to traditional chemotherapy and radiotherapy (1). For chemotherapy, the effect of hypoxia on induced

genes and the change in cell environment often render chemotherapeutic agents ineffective (2–5). In radiation therapy, the presence of oxygen enhances cell killing, and therefore the lack of oxygen in hypoxic cells severely compromises the lethal effects of radiation (2,3). Tumor hypoxia has also been related to an increase in malignant progression by promoting angiogenesis (6) and predisposing tumors to metastasize (7). Hypoxia in a solid tumor can therefore seriously undermine the effectiveness of conventional anti-cancer therapies. To help plan effective treatments, a non-invasive, quantitative PET imaging agent capable of measuring tumor hypoxia before implementation of a treatment regimen would be desirable.

Copper-diacetyl-bis(*N*<sup>4</sup>-methylthiosemicarbazone) ([Cu-ATSM] Fig. 1) has been examined extensively by our group and others as a possible imaging agent to delineate hypoxia within tumors (8–10) and as an agent for radiotherapy (11). It has also been investigated as an agent for the detection of ischemic myocardium (9,12,13). Cu-ATSM is a neutral and lipophilic copper(II)bis(thiosemicarbazone) that has shown rapid diffusion into cells and has been shown *in vitro* to be highly selective for hypoxic tissues (10,14,15). Preliminary clinical studies with <sup>60</sup>Cu-ATSM PET have shown this agent to be a promising, noninvasive, selective diagnostic marker for hypoxia in human cancers (16–19).

Positron-emitting isotopes of copper with high specific activity can be produced on a biomedical cyclotron (20,21). These isotopes are <sup>60</sup>Cu (t<sub>1/2</sub>, 23.7 min; β<sup>+</sup>, 93%; electron capture [EC], 7%), <sup>61</sup>Cu (t<sub>1/2</sub>, 3.33 h; β<sup>+</sup>, 61%; EC, 39%), and <sup>64</sup>Cu (t<sub>1/2</sub>, 12.7 h; β<sup>+</sup>, 17.4%; EC, 43%). The availability of these copper radionuclides allowed us to undertake this investigation to confirm the hypoxic selectivity of Cu-ATSM *in vivo* in an animal tumor model. The oxygen concentration (pO<sub>2</sub>) within the implanted tumors was manipulated by chemical means or by alteration of the inhaled oxygen content. Chemical manipulation was achieved using the vasodilator hydralazine. Hydralazine increases blood flow to organs in the body, but it has been shown to decrease blood flow to tumors; as a result, tumor oxygenation is dramatically decreased for a few hours (22–24). The hypoxia selectivity of Cu-ATSM in these studies was shown

---

Received Jul. 24, 2000; revision accepted Nov. 17, 2000.

For correspondence or reprints contact: Michael J. Welch, PhD, Mallinckrodt Institute of Radiology, Washington University School of Medicine, Campus Box 8225, 510 S. Kingshighway Blvd., St. Louis, MO 63110.

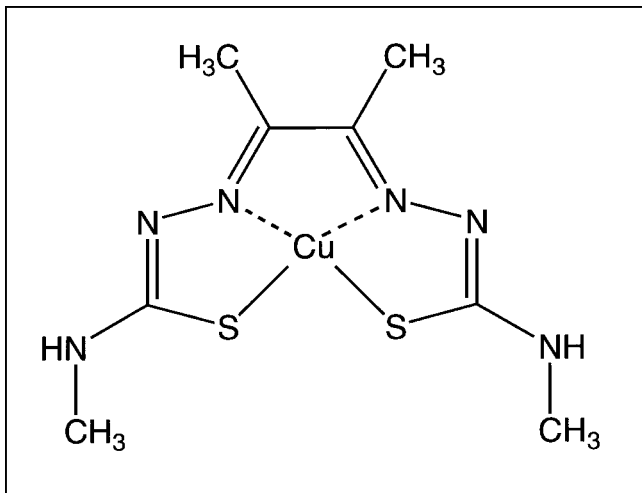


FIGURE 1. Structure of Cu-ATSM.

using a range of techniques, including direct  $pO_2$  assessment using a needle oxygen electrode, electronic autoradiography, and PET.

## MATERIALS AND METHODS

$^{61}Cu$  and  $^{64}Cu$  were produced on a CS-15 biomedical cyclotron (Cyclotron Corp.) at Washington University of School of Medicine using previously reported methods (20,21). For studies requiring longer-lived radionuclides,  $^{67}Cu$  ( $t_{1/2}$ , 62 h;  $\beta^-$ , 100%) was purchased from the U.S. Department of Energy (c/o Brookhaven National Laboratory, Upton, NY). Unless stated otherwise, all chemicals were purchased from Sigma-Aldrich Chemical Co., Inc. (Milwaukee, WI). All solutions were prepared using distilled deionized water (Milli-Q Bedford, MA;  $>18 M\Omega$  resistivity).  $^{64}Cu$ -ATSM,  $^{61}Cu$ -ATSM, and  $^{67}Cu$ -ATSM with  $>98\%$  radiochemical purity were produced by methods described in the literature (8,25).

### Animal Models

All animal experiments were conducted in compliance with the Guidelines for the Care and Use of Research Animals established by Washington University's Animal Studies Committee. Female Fischer 344 rats (150–165 g), purchased from Charles River Laboratories (Wilmington, MA), were implanted subcutaneously with  $1 \times 10^7$  9L gliosarcoma cells in the right flank and were used at day 16 of tumor growth (4–6 g). The 9L cells were a gift from the Brain Tumor Research Center (University of California, San Francisco). All animals were anesthetized with an intraperitoneal injection of 75 mg/kg K-Ketaset (ketamine HCl, USP; Fort Dodge Laboratories, Inc., Fort Dodge, IA) and 0.5 mg/kg Domitor (medetomidine HCl; Pfizer Animal Health, Exton, PA). In autoradiography and PET studies, animals were intubated and ventilated (15 mL/kg tidal volume) with the required oxygen content using a forced-air room-air ventilator (Harvard Apparatus, Holliston, MA). Animals were ventilated on room air unless stated otherwise. In all hydralazine-treated animals, the drug (5 mg/kg in saline [1 mg/mL]) was administered intraperitoneally 1 h before radioactivity administration.

### Determination of Tissue Oxygenation

To measure tissue oxygenation directly, a chemical microsensor (Diamond General Corp., Ann Arbor, MI) was equipped with a

combination 21-gauge needle oxygen electrode (Diamond General Corp., Ann Arbor, MI). The combination needle electrode is a polarographic oxygen electrode with an internal reference. This system is similar to the Eppendorf microelectrode system (KIMOC 6650; Eppendorf, Hamburg, Germany) and measures a similar range of oxygen concentrations. Following manufacturer instructions for calibration, the system was calibrated for 0–5%  $O_2$ , which is appropriate for the level of tissue oxygenation in the 9L tumor. After the required pretreatments, tumors were exposed through a skin flap on the thigh. The needle was inserted into the exposed tumor and allowed to equilibrate for 2 min. The needle was then advanced in 1-mm increments, and readings were taken every 5 s. The needle was slightly withdrawn after each advance to release pressure on the electrode. The needle was advanced along 10–14 tracks through the tumor so that measurements were obtained from a representative tumor volume. A minimum of 100 readings was taken in each tumor. After the final reading, the electrode was recalibrated to ensure correct calibration and cleaned in deionized water to remove salts from the membrane. Histograms were generated on the frequency of  $pO_2$  measurements.

### Electronic Autoradiography

Electronic autoradiography was performed on an InstantImager system (Packard Instrument Co., Meriden, CT). Three groups of animals ( $n = 3$ ) were examined: pretreated hydralazine, saline, and ventilated on an inspired oxygen fraction ( $F_I O_2$ ) of 100% oxygen. In the hydralazine-treated animals, the drug was administered intraperitoneally 1 h before the radioactivity. For the animals ventilated with 100% oxygen, the animals breathed the required atmosphere for 5 min before administration of radioactivity. Each animal was administered 3.7 MBq (100  $\mu Ci$ ) of  $^{67}Cu$ -ATSM through the femoral vein. At 5 min after injection of  $^{67}Cu$ -ATSM, the tumors were exposed, and the needle oxygen electrode was used as described previously for the next 5 min. At 10 min after injection of  $^{67}Cu$ -ATSM, the animals were killed by cervical dislocation. Tumors of similar size were sliced and prepared in Tissue-Tek embedding medium (Miles, Inc., Elkhart, IN). Slices (1 mm thick) were mounted and placed in the InstantImager (Packard) to visualize the distribution of  $^{67}Cu$ -ATSM. Software analysis of the autoradiographs yielded the cpm/mm<sup>2</sup> of radioactivity in each tumor slice. Regions of interest (ROIs) were drawn to encompass each slice, and the total tumor activity was determined by summing all ROI values.

In a separate experiment, a comparison was made between the distribution of  $^{18}F$ -FDG and that of  $^{64}Cu$ -ATSM. In this study, Fischer rats ( $n = 3$ ) bearing 16-d-old 9L tumors were kept fasting 24 h before the experiment. Each rat received an intravenous injection of 37 MBq (1 mCi) FDG followed 50 min later by 1.85 MBq (50  $\mu Ci$ )  $^{64}Cu$ -ATSM. The animals were killed 60 min after injection of FDG (10 min after injection of  $^{64}Cu$ -ATSM), and the tumors were excised and sliced as described previously. Autoradiography of the slices initially visualized the FDG (1-h distribution) and was repeated 24 h later to visualize the  $^{64}Cu$ -ATSM (10-min distribution). Standard radioisotope mixtures were also made and imaged to ensure that  $>99.9\%$  of the initial image was generated by the  $^{18}F$  and that only  $^{64}Cu$  images remained in the 24-h images.

### PET

PET was performed on an ECAT EXACT HR<sup>+</sup> scanner (Siemens/CTI, Knoxville, TN). Four 9L-bearing animals were anesthetized and placed supine in the scanner in a support of our own

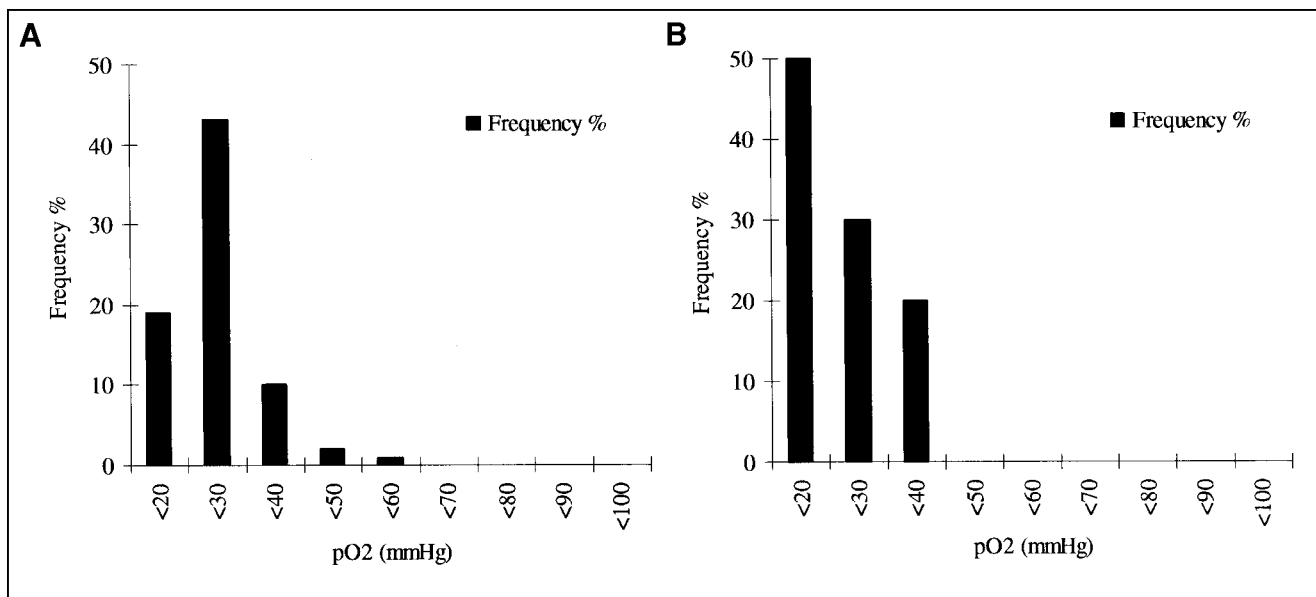


**FIGURE 2.** Oxygen probe evaluation of 9L tumors in age-matched rats. (A) Representative oxygenation of tumor in normal untreated animal. (B) Representative oxygenation of tumor in rat that received hydralazine 1 h before pO<sub>2</sub> measurements.

design, and a jugular cut was performed to administer radiopharmaceuticals through the jugular vein. The animals were then treated with F<sub>1</sub>O<sub>2</sub> of 10% oxygen 5 min before <sup>61</sup>Cu-ATSM, F<sub>1</sub>O<sub>2</sub> of 100% oxygen 5 min before <sup>61</sup>Cu-ATSM, hydralazine 60 min before <sup>61</sup>Cu-ATSM, or saline 60 min before <sup>61</sup>Cu-ATSM. A 15-min attenuation scan was performed before administration of <sup>61</sup>Cu-ATSM (32.0–36.1 MBq [865–975 μCi] per animal) as a bolus injection, followed by 25 min of dynamic data collection (20 × 5-s frames, 6 × 30-s frames, 20 × 60-s frames). Time-activity curves (TACs) were generated from ROIs drawn to encompass the entire tumor.

## RESULTS

Hydralazine administration decreased the average tumor pO<sub>2</sub> from 28.61 ± 8.74 mm Hg to 20.81 ± 7.54 mm Hg in

control animals (Fig. 2). It also increased the relative tumor uptake of <sup>67</sup>Cu-ATSM by 37% (*P* < 0.001) compared with the control animals (1.37 ± 0.35 vs. 1.00 ± 0.40) (Fig. 3). Conversely, in animals administered 100% oxygen, the average tumor pO<sub>2</sub> increased to 45.88 ± 15.9 mm Hg, and the tumor <sup>67</sup>Cu-ATSM uptake decreased to just 48% of the control animals (0.48 ± 0.30) (*P* < 0.001). Autoradiography also provided clear visual evidence of the preferential uptake of <sup>67</sup>Cu-ATSM in hypoxic tissue. Hydralazine-treated tumors had higher uptake than those from animals treated with 100% oxygen (Fig. 4A vs. B), whereas control (saline treated) tumors showed a range of tumor oxygenation (Fig. 4C).

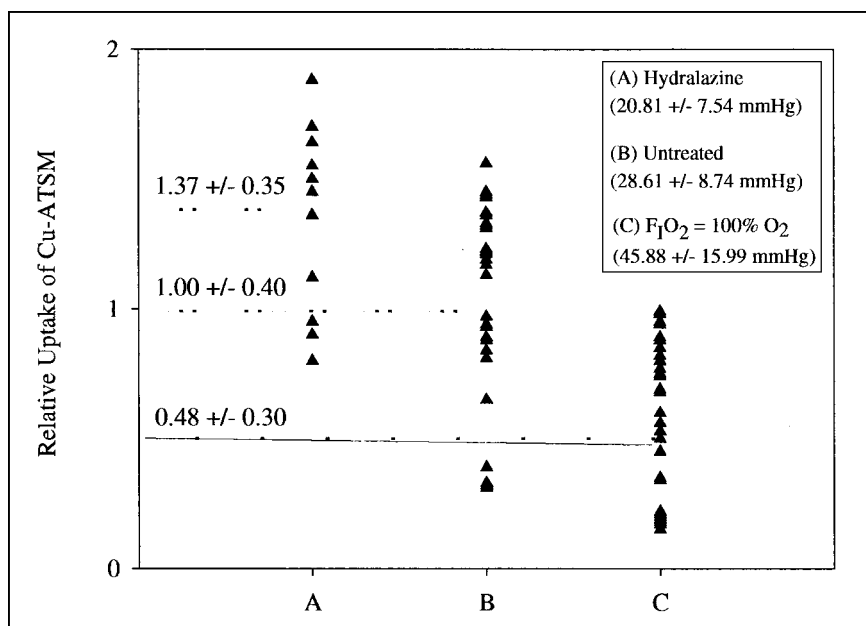


**FIGURE 3.** Correlation of <sup>67</sup>Cu-ATSM uptake with oxygen probe measurements in 9L tumors subjected to various degrees of oxygenation (same animals as in Fig. 4). Relative uptake was determined by quantification of <sup>67</sup>Cu-ATSM in 1-mm tumor slices using InstantImager (Packard Instrument Co., Meriden, CT). Oxygen measurements were taken 5 min after injection of <sup>67</sup>Cu-ATSM; kill was performed 10 min after tracer injection. Hydralazine-treated animals showed significantly higher uptake of <sup>67</sup>Cu-ATSM (A, average pO<sub>2</sub> = 20.81 ± 7.54 mm Hg, *n* = 3) than did well-oxygenated animals (C, average pO<sub>2</sub> = 45.88 ± 15.99 mm Hg, *n* = 3). Tumors from control animals showed wide range of <sup>67</sup>Cu-ATSM uptake (B, average pO<sub>2</sub> = 28.61 ± 8.74 mm Hg, *n* = 3).

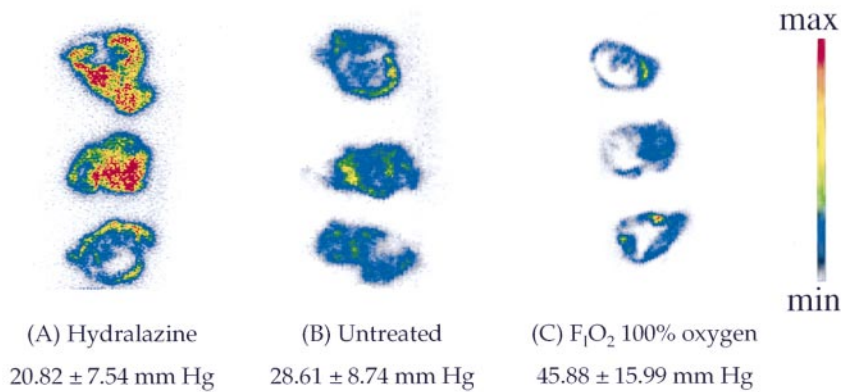


**FIGURE 4.** Typical autoradiographs of  $^{67}\text{Cu}$ -ATSM distribution in 9L tumors with manipulated oxygenation levels. Tumors used were of comparative size, and slices were selected at random from tumors shown in Figures 2 and 3. The hydralazine-treated animals visually show higher uptake of  $^{67}\text{Cu}$ -ATSM (A) compared with well-oxygenated animals (C). Control untreated tumors show wide range of  $^{67}\text{Cu}$ -ATSM uptake (B). White areas of very low uptake seen within tumors were examined visually and were not necrotic.

In autoradiographic studies comparing the distribution of FDG and  $^{64}\text{Cu}$ -ATSM in the same animal, we found regions of increased uptake of  $^{64}\text{Cu}$ -ATSM that are distinctly different from regions of increased FDG uptake. Early images of typical tumor slices indicated clear regional uptake of FDG on the left-hand side of the tumor (Fig. 5, left), whereas images of the same slices after  $^{18}\text{F}$  fully decayed showed  $^{64}\text{Cu}$ -ATSM localized elsewhere (Fig. 5, right).

Analysis of the data from PET showed a rapid uptake of  $^{61}\text{Cu}$ -ATSM in all tumors (Fig. 6), with peak values noted at 80 s after tracer administration, regardless of the experimental treatment. In the 10% oxygenated tumor, uptake gradually declined from a peak of 2.96% injected activity (IA) at 80 s to a final value of 2.22% IA at 25 min. In the 100% oxygenated tumor, a peak of 2.28% IA at 80 s fell dramatically, because only 1.45% IA remained at 25 min after injection, a value nearly 40% less than that in the 10% oxygenated tumor. In the hydralazine-treated tumor,  $^{61}\text{Cu}$ -

ATSM was retained in the tumor over the course of imaging. Although the hydralazine-treated tumor had the lowest peak uptake (2.05% IA at 80 s), the uptake was still 2.06% IA at 25 min, comparable with the saline and 10% oxygenated tumors and much higher than the 100% oxygenated tumor. The saline control tumor had a rapid initial uptake of the tracer (2.68% IA at 80 s) and then declined to a low of 1.93% IA at 15 min, after which uptake slowly increased to 2.13% IA at 25 min.

## DISCUSSION

Because tumor oxygenation is a key factor in the success or failure of radiotherapy and chemotherapy, determining the hypoxic fraction within a tumor is an important goal.  $\text{Cu(II)-ATSM}$  is a complex of low molecular weight and high membrane permeability that has shown selective retention within hypoxic cells *in vitro* (10,14). Currently,

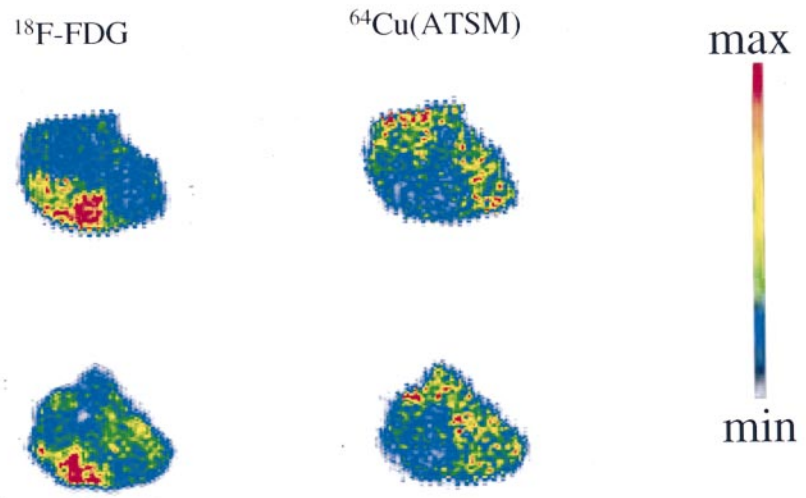


**FIGURE 5.** Typical dual-tracer autoradiograph of two slices of 9L tumor from fasted but otherwise untreated rat, with FDG distribution at 60 min after injection (imaged shortly after kill, left) and  $^{64}\text{Cu}$ -ATSM distribution at 10 min after injection (imaged 24 h after kill, right). Difference in regional uptake between tracers is seen clearly.

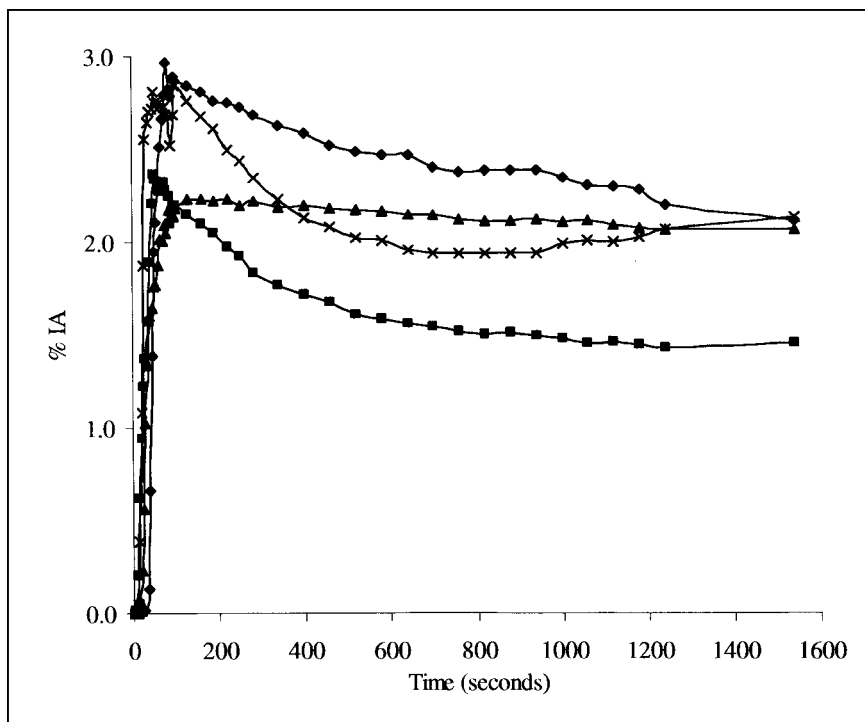


**FIGURE 6.** Time-activity curves generated by drawing ROIs over tumors from  $^{61}\text{Cu}$ -ATSM PET of rats bearing 9L tumors under varying degrees of oxygenation. Data are normalized to amount of radioactivity injected. ◆,  $\text{F}_1\text{O}_2$  10% oxygen:90% nitrogen; ■,  $\text{F}_1\text{O}_2$  100% oxygen; ▲, hydralazine; ×, saline.

$^{60}\text{Cu}$ -ATSM is being evaluated as an agent for the detection of viable hypoxic tumor tissue in humans using PET (17–19) and as an agent for the demarcation of ischemic myocardium (12,13). Studies conducted using the Langendorff model of an isolated and perfused rat heart, in which the oxygen concentration can be controlled, showed that the specific retention of Cu-ATSM was caused by oxygen depletion (8,9). In rat myocardium,  $^{64}\text{Cu}$ -ATSM was rapidly washed out from normally perfused, isolated rat hearts, whereas ischemic hearts had 3.5-fold greater uptake of tracer by 15 min after injection (8). It has been proposed that the selectivity of Cu-ATSM for hypoxic tissue is caused partly by its redox potential of  $-293$  mV, which enables more Cu-ATSM to be reduced in hypoxic cells than in normal cells (8–10). Although in vitro studies showed Cu-ATSM collects selectively in hypoxic cells, and in vivo evidence hinted at a similar finding, we undertook this study to confirm the relationship between Cu-ATSM uptake and  $\text{pO}_2$  in vivo. We report the selectivity of Cu-ATSM for hypoxic tissue in vivo by correlating direct measurements of tumor oxygenation with autoradiography and PET in a tumor-bearing animal model.

The reported transient induction of hypoxia by hydralazine in tumor tissue was verified by oxygen probe measurements, which showed a significantly lower average tumor  $\text{pO}_2$  for hydralazine-treated animals than for control animals ( $20.81 \pm 7.54$  mm Hg vs.  $28.61 \pm 8.74$  mm Hg) (Fig. 2). As expected, tumor oxygenation was dramatically higher in the intubated rats administered an  $\text{F}_1\text{O}_2$  of 100% before tracer injection (average tumor  $\text{pO}_2$ ,  $45.88 \pm 15.99$  mm Hg). The average tumor oxygenation in the hydrala-

zine-treated animal was significantly different from the 100% oxygenated animal ( $P < 0.001$ ), whereas the untreated control group showed an average  $\text{pO}_2$  consistent within a mixture of tissue oxygenations ( $28.61 \pm 8.74$  mm Hg). Thus, hydralazine can dramatically manipulate the dissolved oxygen levels within tumor tissue in this animal model.

The tissue uptake of Cu-ATSM in the 9L tumors was measured using the InstantImager (Packard), which was shown previously to exhibit linearity over a wide range of counting rates for the radionuclides used, making it an ideal instrument for ex vivo imaging of radionuclides of different half-lives (9,10). The relative uptake in each group of animals was normalized to the average uptake of the tracer in the control animals. The oxygenated animals showed a tracer uptake of less than half of that in the saline-treated control animals and only one third of that in the hydralazine-treated animals. The hydralazine-treated animals exhibited a 1.3-fold increase in uptake compared with the control animals. These differences in uptake can be seen in Figure 4. In the hydralazine-treated animals, high uptake in the tumor mass was fairly uniform over the whole tumor (Fig. 4A). In untreated animals, the tracer uptake was more modest and heterogeneous (Fig. 4B), consistent with the presence of oxygenated and hypoxic zones in the tumor, an observation proved by direct  $\text{pO}_2$  measurements (Fig. 2). The well-oxygenated tumor showed very little uptake of the tracer (Fig. 4C), consistent with high levels of  $\text{pO}_2$ .

Although the average tumor  $\text{pO}_2$  was statistically different between each experimental group, appreciable overlap occurred between the groups. Heterogeneity of tumor  $\text{pO}_2$  is

a recognized limitation of oxygen probe measurements and shows that a large, statistically relevant dataset must be collected. A recent study showed that tumor  $pO_2$  fluctuates rapidly within tumors naturally (26). This heterogeneity does not preclude the usefulness of the measurement technique, but it is a potentially limiting factor. It is possible that the diagnostic use of Cu-ATSM could be limited by oxygenation heterogeneity, a problem for all potential hypoxic markers. However, the kinetics of Cu-ATSM and the target-tissue-to-background ratios achieved are superior to other tracers, improving its chances of being clinically useful. Kinetic models of this tracer in human neoplasms are being developed to overcome the problem of tumor tissue  $pO_2$  heterogeneity (18). Another attractive option would be to correlate the  $pO_2$  measurement in a particular position with the relative uptake of Cu-ATSM at that position. However, current attempts to do so have been unsatisfactory. In future studies, we propose to correlate Cu-ATSM PET with  $O_2$  saturation measurements in animals by using a computer-assisted stereotactic electrographic probe currently in development.

Dual-tracer ex vivo autoradiography was performed by injecting FDG and  $^{64}Cu$ -ATSM into the same animal. The validation of dual-tracer experiments with the InstantImager (Packard) has been reported (9). In some tumor slices, a clear demarcation was observed (Fig. 5), indicating that FDG and  $^{64}Cu$ -ATSM localized in different regions. In these slices, it is tempting to conclude that in 9L tumors, regions of high metabolism (shown by FDG) are not very hypoxic (shown by the  $^{64}Cu$ -ATSM image) and vice versa. However, it is reasonable and possible for regions of high FDG uptake to also show high Cu-ATSM uptake, and other slices showed as much (data not shown). In the tumor microenvironment, tumor cells in close proximity to the vasculature would presumably have high FDG uptake, whereas cells remote from the vascular bed could be hypoxic and therefore have high Cu-ATSM uptake. The difference between these locations could be less than the image resolution, leading to an observed overlap of FDG and Cu-ATSM, and high metabolism and hypoxia could also exist within the same tumor cell. Similarly, demarcation might reflect blood flow differences rather than metabolism and oxygenation differences. Therefore, when considering the relationship between regions of high metabolism and hypoxia, it is important to remember that several situations can exist.

The PET experiment described in this study is most similar to the clinical situation, in which data collection and analysis are done in vivo. However, in this experiment we manipulated the oxygenation status of each tumor to create tumor environments of high oxygenation or hypoxia. Close examination of the data (Fig. 6) shows a rapid initial uptake of the tracer, peaking at 80 s, independent of the oxygenation status. These peak uptake values differ, however, and when normalized to the amount of radioactivity injected, they are ordered as follows:  $F_1O_2$  10% > normal >  $F_1O_2$

100% > hydralazine. This order is consistent with the expected physiologic changes in blood flow resulting from each intervention: low atmospheric oxygen increases the heart rate and blood pressure; oxygen concentrations higher than normal decrease the heart rate and blood pressure; and hydralazine decreases the blood flow to tumors even as it increases the blood flow to normal tissues. The peak values of the TACs are indicative of blood flow and hence the initial delivery of the tracer. The two hypoxic groups ( $F_1O_2$  10% and hydralazine) exhibited very different peak values, and that for hydralazine was lower. This result could be caused by hydralazine affecting the blood flow of other tissues.

It is, however, the retention of Cu-ATSM, rather than its initial delivery to the tumor, that should best depict tumor oxygenation, because hypoxic cells are more able to reduce and trap Cu-ATSM. For example, the 100% oxygenated tumor had approximately 1.5 times less tracer than the hypoxic tumors and the control group after 25 min, despite having a higher peak value. Interestingly, the hydralazine-treated animal, although having a lower peak uptake value at 80 s, had the greatest retention and highest uptake at 25 min; that is, all radioactivity initially delivered was retained over the 25-min examination period. Not only have we directly measured tumor  $pO_2$  and verified that hydralazine can significantly reduce tumor oxygenation, but we also confirmed its proposed mechanism of action, whereby tumor hypoxia stems from increased blood flow to normal tissues and decreased blood flow to tumors (22–24). Our data show that hydralazine-treated animals have a lower peak uptake value, reflecting reduced flow, and also complete retention of Cu-ATSM in the tumor, indicating a large hypoxic fraction. In these hydralazine experiments, the opposing effects of reduced blood flow and increased hypoxia on tracer distribution resulted in higher Cu-ATSM uptake at 25 min than for other experimental groups. These PET data clearly support the oxygen probe and autoradiography data, confirming the selectivity of Cu-ATSM for hypoxic tissues.

The differences in uptake between normal and hypoxic tumor tissue (1:1.5) are not as high as those observed in the Langendorff model of an isolated and perfused rat heart (1:3.5) (8). In the Langendorff model, the oxygen concentration can be controlled without any changes in flow rates or substrate supply. These potential confounding factors may account for the smaller differences in uptake seen in the tumor data presented here, where flow and thus substrate delivery are affected and cannot be controlled. The difference between uptake in hypoxic tissue and that in oxygenated tissue may still, however, be high enough for efficient hypoxia delineation with Cu-ATSM PET for humans, although further validation in humans is required.

## CONCLUSION

These data confirm the hypothesis that Cu-ATSM retention in tissue in vivo is dependent on tissue  $pO_2$  and that

greater retention of this tracer occurs in hypoxic tissue. This finding validates the current use of  $^{60}\text{Cu}$ -ATSM and PET as a clinical tool to ascertain the hypoxic fraction of human tumors. The ultimate goal is to use  $^{60}\text{Cu}$ -ATSM to determine tumor hypoxia and to act as a prognostic indicator to help plan the most effective and potentially successful treatment.

## ACKNOWLEDGMENTS

The authors thank Dr. Mark A. Mintun for helpful discussions; Dr. Deborah McCarthy and Todd A. Perkins for the production of  $^{61/64}\text{Cu}$ ; and John Engelbach, Mark Nolte, Margaret Morris, and Lynne Jones for technical assistance. The authors also thank Dr. Joanna B. Downer for editorial assistance. This study was supported by the U.S. Department of Energy (DE-FG02-87ER60512). The production of copper radionuclides at Washington University was supported by a grant from the National Cancer Institute (1 R24 CA86307).

## REFERENCES

- Brown JM. The hypoxic cell: a target for selective cancer therapy—Eighteenth Bruce F. Cain Memorial Award Lecture. *Cancer Res.* 1999;59:5863–5870.
- Crabtree HG, Cramer W. The action of radium on cancer cells I. II. Some factors determining the susceptibility of cancer cells to radium. *Proc R Soc Ser B.* 1933;113:238–250.
- Gray LH, Conger AD, Ebert M, Hornsey S, Scott OC. Concentration of oxygen dissolved in tissues at the time of irradiation as a factor in radiotherapy. *Br J Radiol.* 1953;26:638–648.
- Tannock I, Guttman P. Responses of Chinese hamster ovary cells to anticancer drugs under aerobic and hypoxic conditions. *Br J Cancer.* 1981;42:245–248.
- Teicher BA, Holden SA, Al-Achi SA, Herman TS. Classification of antineoplastic treatments by their differential toxicity toward putative oxygenated and hypoxic tumor subpopulations *in vivo* in the FSaIIc murine fibrosarcoma. *Cancer Res.* 1990;50:3339–3344.
- Shweiki D, Itin A, Soffer D, Keshet E. Vascular endothelial growth factor induced by hypoxia may mediate hypoxia-initiated angiogenesis. *Nature (Lond).* 1992;359:843–845.
- Graeber TG, Osmanian C, Jacks T, et al. Hypoxia-mediated selection of cells with diminished apoptotic potential in solid tumours. *Nature (Lond).* 1996;379:88–91.
- Fujibayashi Y, Taniuchi H, Yonekura Y, Ohtani H, Konishi J, Yokoyama A. Copper-62-ATSM: a new hypoxia imaging agent with high membrane permeability and low redox potential. *J Nucl Med.* 1997;38:1155–1160.
- Fujibayashi Y, Cutler CS, Anderson CJ, et al. Comparative imaging studies of  $^{64}\text{Cu}$ -ATSM a hypoxia imaging agent and C-11-acetate in an acute myocardial infarction model: ex vivo imaging in rats. *Nucl Med Biol.* 1999;26:117–121.
- Lewis JS, McCarthy DW, McCarthy TJ, Fujibayashi Y, Welch MJ. Evaluation of  $^{64}\text{Cu}$ -ATSM in vivo and in vitro in a hypoxic tumor model. *J Nucl Med.* 1999;40:177–183.
- Lewis JS, Laforest R, Buettner TL, et al. Copper-64-diacetyl-bis(*N*<sup>4</sup>-methylthiosemicarbazone): an agent for radiotherapy. *Proc Natl Acad Sci USA.* 2001;98:1206–1211.
- Welch MJ, Lewis JS, McCarthy DW, Sharp T, Herrero P, Fujibayashi Y. Evaluation of copper-60-diacetyl-bis(*N*<sup>4</sup>-methylthiosemicarbazone) (Cu-ATSM), a hypoxia imaging agent, in canine models of ischemia [abstract]. *Eur J Nucl Med.* 1988;25:920.
- Sharp TL, Lewis JS, Herrero P, et al. Quantification of Cu-ATSM kinetics by compartmental modeling in normal, ischemic and necrotic myocardium [abstract]. *J Nucl Med.* 2000;41:175.
- Dearling JJJ, Lewis JS, Mullen GED, Welch MJ, Blower PJ. Design of hypoxia-targeting radiopharmaceuticals: selective uptake of copper-64 complexes in hypoxic cells in vitro. *Eur J Nucl Med.* 1998;25:788–792.
- Dearling JJJ, Lewis JS, Welch MJ, McCarthy DW, Blower PJ. Redox-active complexes for imaging hypoxic tissues: structure-activity relationships in copper(II)bis(thiosemicarbazone) complexes. *Chem Commun.* 1998;22:2531–2533.
- Takahashi N, Fujibayashi Y, Yonekura Y, et al. Evaluation of copper-62 ATSM in patients with lung cancer as a hypoxic tissue tracer [abstract]. *J Nucl Med.* 1998;39:53.
- Dehdashti F, Mintun MA, Lewis JS, Govindan R, Welch MJ. Evaluation of tumor hypoxia with Cu-60-ATSM and PET [abstract]. *J Nucl Med.* 2000;41:34.
- Mintun MA, Berger KL, Dehdashti F, Lewis JS, Chao C, Welch MJ. Kinetic analysis of the novel hypoxic imaging agent [ $^{60}\text{Cu}$ ]ATSM in human neoplasms [abstract]. *J Nucl Med.* 2000;41:58.
- Chao C, Bosch WR, Mutic S, et al. An approach to hypoxic PET guided conformal radiation therapy [abstract]. *J Nucl Med.* 2000;41:284.
- McCarthy DW, Shefer RE, Klinkowstein RE, et al. Efficient production of high specific activity  $^{64}\text{Cu}$  using a biomedical cyclotron. *Nucl Med Biol.* 1997;24:35–43.
- McCarthy DW, Bass LA, Cutler PD, et al. High purity production and potential applications of copper-60 and copper-61. *Nucl Med Biol.* 1999;26:351–358.
- Chaplin DJ, Acker B. The effect of hydralazine on the tumor cytotoxicity of the cell cytotoxin RSU 1069: evidence for therapeutic gain. *Int J Radiat Oncol Biol Phys.* 1987;13:579–585.
- Chaplin DJ. Hydralazine-induced tumor hypoxia: a potential target for cancer chemotherapy. *J Natl Cancer Inst.* 1989;81:618–622.
- Voorhees WD, Babbs CF. Hydralazine enhanced selective heating of transmissible venereal tumor implants in drugs. *Eur J Cancer Clin Oncol.* 1982;19:1027–1033.
- Young H, Carnochan P, Zweit J, Babich J, Cherry S, Ott R. Evaluation of copper(II)-pyruvaldehyde bis(*N*<sup>4</sup>-methylthiosemicarbazone) for tissue blood flow measurement using a trapped tracer model. *J Nucl Med.* 1994;21:336–341.
- Braun RD, Lanzen JL, Dewhirst MW. Fourier analysis of fluctuations of oxygen tension and blood flow in R3230Ac tumors and muscle in rats. *Am J Physiol.* 1999;277:H551–568.